http://dx.doi.org/10.5012/bkcs.2011.32.10.3581

Positively Charged Silver Nanoparticles Threaded on Carbon Nanotube for the Efficient Delivery of Negatively Charged Biomolecules

Hyung-Seok Park,[†] Ji-Young Hwang,[‡] Ueon Sang Shin,[†,‡] Hae-Won Kim,[†,‡,§] and Myoung-Seon Gong[†,‡,*]

[†]*Department of Nanobiomedical Science & WCU Research Center, Dankook University Graduate School, Chungnam 330-714, Korea.* [*]*E-mail: msgong@dankook.ac.kr*
[‡]*Institute of Tissue Regeneration Engineering (ITREN), Dankook University, Chungnam 330-714, Korea*
[§]*Department of Biomaterials Science, School of Dentistry, Dankook University, Chungnam 330-714, Korea*
Received March 28, 2011, Accepted August 5, 2011

Silver nanoparticle (Ag-NPs)-immobilized and amine-functionalized carbon nanotubes (MWCNTs), MWCNT-Ag-NH_2, were easily prepared in order to develop an efficient delivery system of biomolecules without complicated processes of manufacture. For this, Ag-NPs-immobilized MWCNTs, MWCNT-Ag, were initially prepared in order to create large surface area to enable more efficient linkage with guest-molecules using pristine MWCNTs. The Ag-NPs on MWCNTs were further positively functionalized with 2-aminoethanthiol to allow ionic linkage with biomolecules. Ultimately, the positively charged delivery system proved to be highly effective for the binding capacity of bovine serum albumin (BSA) as a negatively charged model protein, when compared to that of lysozyme used as a positively charged model protein. The releasing profile of BSA was observed in almost linear pattern for about two weeks in a saline solution. This study demonstrated the potential usefulness of the pristine MWCNTs in conjunction with Ag-NPs for the selective delivery of many (negatively or positively) charged biomolecules including proteins and genes.

Key Words : Carbon nanotubes, Silver nanoparticle, Positively charged nanohybrid

Introduction

Nanotechnology offers many potential advantages to the design of drug delivery systems. The manufacturing process and the surface properties of the system as a nanotemplate have a significant impact on the efficiency for drug delivery. Due to their interesting structural and physicochemical properties, including high aspect ratio and relatively easy surface modification, carbon nanotubes (CNTs) have been well known as an attractive nanotemplate to develop for use in controlled and targeted drug delivery.[1-3] The chemically-inert surface of CNTs often has been functionalized with strong oxidants in strong acid to gain more efficient link with amine- or thiol-sites of biomolecules, resulting in the formation of carboxyl groups intensively at the end of CNT tubes (CNT-COOH) with severe damage.[4-12] Further functionalization of the carboxyl groups on modified CNTs was also attempted to increase the adhesion efficacy of proteins.[6,7] However the functionalization of CNTs has been showing the limit to increase the efficiency of the protein delivery, because it may be difficult that the whole surface of CNTs is uniformly to be functionalized. To increase surface area of drug templates and to gain more efficient link with protein molecules, metallic nanoparticles functionalized with various methods were also employed as drug delivery system. To maximize the loading capacity of biomolecules, methods to combine metallic nanoparticles with CNTs have recently been developed.[13] Especially, the integration of silver nanoparticles (Ag-NPs) with CNTs is considered to be of special merit due to the additional biological function of Ag-NPs, including antimicrobial activity.[12,14,15] Moreover, great attention has recently been given to the surface-functionalized Ag-NPs in order to develop them as a delivery system of drugs, genetic materials and diagnostic agents .[16-20]

In this study, we newly designed an efficient delivery system of biomolecules by combining unfunctionalized MWCNTs with functionalized Ag-NPs. For this, Ag-NPs was initially immobilized onto the surface of pristine MWCNTs by facile reduction of silver alkylcarbamate complex,[21-29] following amine-functionalization of the Ag-NPs to allow binding of biomolecules such as proteins and genes. The positively charged delivery system ultimately proved to be highly effective for the binding capacity of bovine serum albumin (BSA) as a negatively charged model protein, when compared to that of lysozyme used as a positively charged model protein. The releasing profile of BSA was observed in almost linear pattern for about two weeks in a saline solution.

Experimental Section

Materials and Instruments. Pristine multi-walled carbon nanotubes synthesized by chemical vapor deposition were purchased from ILJIN Nanotech Co., Ltd. (Seoul, Korea). Ag-Ink (an isopropyl alcohol (IPA) solution of silver(I) complex with 2-ethylhexyl amine and 2-ethylhexylammonium carbamate; Ag = 10 wt %) was purchased from InkTec Co., Ltd., Korea and was used as a silver-precursor. Bovine serum albumin (BSA) and lysozyme were purchased from

Sigma-Aldrich and phosphate buffer solution (PBS, pH 7.0) from GIBCO Invitrogen Corporation. All other chemicals including aminoethanthiol and isopropyl alcohol (IPA) were obtained from commercial sources and used without further purification.

Morphological characterization of MWCNTs and Ag-NPs was performed by transmission electron microscopy (TEM) using a JEOL electron microscope (JEM1010). Information about organic functional groups was obtained by Fourier transform infrared spectroscopic (FT-IR) measurements using Biorad Excaliber TS-3000MX spectrophotometer in the range of 4000-800 cm^{-1}. TGA measurements were carried out on a Shimadzu TGA 50 thermal analyzer at a heating rate of 10 °C/min under nitrogen. The XRD pattern of the silver nanoparticle was measured using a Rigaku Ultima IV X-ray diffractometer with the CuKα radiation (λ = 1.54056 Å) at a scanning rate of 2 degrees per second in 2θ ranging from 20° to 90°. UV-vis spectra were obtained using the Shimadzu, UV-1601PC spectrometer over the 200 to 800 nm ranges with 1 nm resolution and background correction using PBS. Zeta (ξ) potential measurement was carried out by means of Zetasizer nano ZS90 (Malvern). The Zeta (ξ) potential of distillation water solutions of containing pristine MWCNTs and the derivatives such as 1-SbF_6, 1-Cl and 1-tartrate were recorded at room temperature. The Zeta (ξ) potential was automatically calculated from electrophoretic mobility based on the Smoluchowski equation, $v = (\varepsilon E/\eta)\xi$, where v is the measured electrophoretic velocity, η is the viscosity, ε is the electrical permittivity of the electrolytic solution and E is the electric field.

Preparation of MWCNT-Ag and MWCNT-Ag-NH_2 Hybrids. 20 mg pristine MWCNTs were stirred in 40 mL Ag-Ink and 160 mL isopropyl alcohol with H_2 gas bubbling for 0.5 and 1 h at room temperature. The Ag-NPs-immobilized MWCNTs (MWCNT-Ag) were separated from the reaction solution by centrifuge, washed with acetone several times and then dried in vacuum. For amine-functionalization of Ag-NPs formed on MWCNTs, the as-prepared MWCNT-Ag complexes and aminoethanthiol were dispersed in isopropyl alcohol with ultrasonic vibration for 5 minutes. The final product was separated from the reaction solution by centrifuge, washed with isopropyl alcohol and acetone several times and then dried in vacuum.

Protein Loading onto MWNT-Ag-NH_2. As the model biomolecule, BSA was used. For comparison study, lysozyme was also used. For the protein loading study, 10 mg MWCNT-Ag-NH_2 powder was dispersed by gentle stirring within the protein solution (10 mg protein) in phosphate buffered saline (PBS) at room temperature and pH 7.0. At regular intervals (1-8 h), the suspension was allowed to be centrifuged at 10000 rpm for 10 min and washed three times to eliminate free protein. The supernatant was subjected to UV-vis spectrometer to measure the amount of proteins adsorbed on MWCNT-Ag-NH_2 via measuring the intensity of absorbance peak at λ_{max} = 278. The resultant MWCNT-Ag-NH_2 hybrid bound with protein was dried under vacuum for further release tests.

Protein Release Kinetics. 1 mg of protein-loaded MWCNT-Ag-NH_2 powder was dissolved in 1 mL of PBS buffer solution (pH = 7.0). After each time period (every 24 h for up to 16 days), the suspension was centrifuged and the supernatant was measured by UV-vis spectrometer at an absorbance of 278 nm. The cumulative release amount and release rate each day were calculated.

Zeta Potential Measurement. 1.5 mg of BSA and lysozyme were dissolved by gentle stirring in 10 mL of distillation water. 1.5 mg of MWCNT-Ag-NH_2 and pristine MWCNT powder were dispersed by sonicator in 20 mL of distillation water. Respectively, the zeta potential values of the suspensions were measured by Zetasizer nano ZS90 (Malvern) at room temperature and pH = 7.0.

Result and Discussion

Ag-NPs-immobilized multi-walled carbon nanotubes, MWCNT-Ag, were prepared from reduction of silver 2-ethylhexylcarbamate complex on MWCNTs with H_2. To create binding sites for biomolecules, Ag-NPs formed on MWCNTs were further modified with aminoethanthiol to produce amine-functionalized (positively charged) MWCNT-Ag nanohybrid, MWCNT-Ag-NH_2. The current design of MWCNT-Ag-NH_2 hybrid as an efficient delivery system of negatively charged biomolecules is schematically shown in Figure 1(a). The surface morphologies of MWCNT-Ag nanohybrids, which were taken after H_2 gas bubbling for 30 and 60 min, were characterized by transmission electron microscopy. As shown Figure 1(b) and (c) (see Figure S1), after 30 min of stirring, Ag-NPs, which are distributed more or less uniformly on the external surface of the MWCNTs, are seen to have a diameter of about 20 nm and a distance of about 100 nm from neighboring particles. When the reduction time increased to 60 min, the size and the density of the nanoparticles grew to up to 50 nm and by 2-3 times, respectively. The MWCNT-Ag hybrid (H_2-bubbled for 60

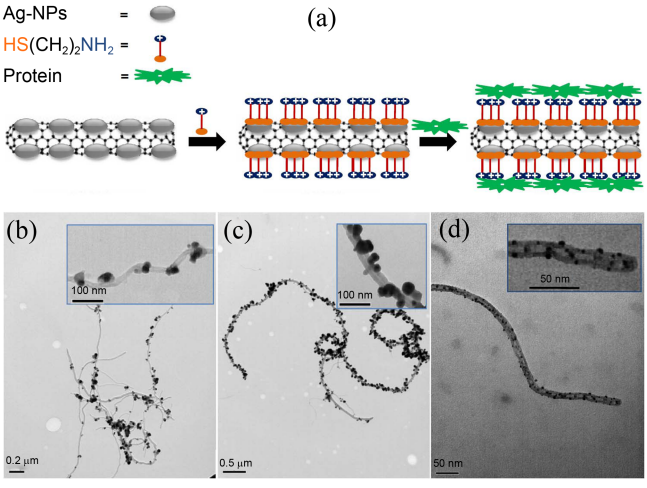

Figure 1. (a) Schematic illustration of the preparation of positively charged nanohybrids (MWCNT-Ag-NH_2) and their use; TEM morphologies of MWCNT-Ag nanocomposites, after reduction for (b) 30 and (c) 60 min, and (d) MWCNT-Ag-NH_2 nanohybrid.

min), with a highly increased surface area, was further functionalized with 2-aminoethanthiol to allow ionic linkage with biomolecules. Figure 1(d) is a TEM image of the MWCNT-Ag-NH_2 hybrids, on which Ag-NPs are distributed more uniformly on the external surface of the MWCNTs. The average diameter of the Ag nanoparticles on MWCNT-Ag-NH_2 hybrids is less than 10 nm, much smaller than the average size of the Ag-NPs initially deposited on the MWCNT-Ag. Large Ag nanoparticles may be detached from the MWCNTs during the modification with aminoethanthiol under ultrasonic vibration, leading to the involvement of much smaller and uniform-sized Ag nanoparticles. The MWCNT-Ag and MWCNT-Ag-NH_2 hybrids were qualitatively characterized using X-ray diffractometer (XRD, Rigaku Ultima IV, CuKα radiation (λ = 1.54056 Å)) (Figure 2(a)-(c)). Figure 2(a) shows the XRD pattern of pristine MWCNTs. The diffraction peaks at 2θ of 26.24° and 42.58° are due to the (002) and (110) planes of MWNTs. Figure 2(b) and 2(c) are the XRD patterns of the MWNT-Ag and MWCNT-Ag-NH_2, respectively. The diffraction peaks at 2θ of 38.00°, 44.4°, 64.5° and 77.5° can be readily indexed to (111), (200), (220), and (310) reflections of silver metal crystals on both hybrid structures, representing the face-centered cubic (fcc) phase of silver. Fourier transform infrared spectroscopy (FT-IR, Biorad Excaliber TS-3000MX) was used to characterize the absorption peaks of the functional groups of aminoethanthiol immobilized on the MWCNT-Ag-NH_2. As shown in Figure 3, the amine group (N-H stretch) and the methylene groups (CH_2 stretch) of aminoethanthiol appeared, centered at about 3480 cm^{-1} and 2850 and 2920 cm^{-1}, respectively. The weak and broad amine-related bands at about 3480 cm^{-1} and two bands for CH_2 stretching vibrations appeared in the rage of 2920-2850 cm^{-1} good testified the successful amine-functionalization of the MWCNT-Ag nanohybrid. Thermo-gravimetric analysis (TGA; Shimadzu TGA 50 thermal analyzer) also showed the existence and the relative amounts of Ag-NPs and aminoethanthiol moiety (Figure 3). The samples were heated from 25 to 900 °C at the rate of 10 °C/min. The MWCNT-Ag hybrid started to be

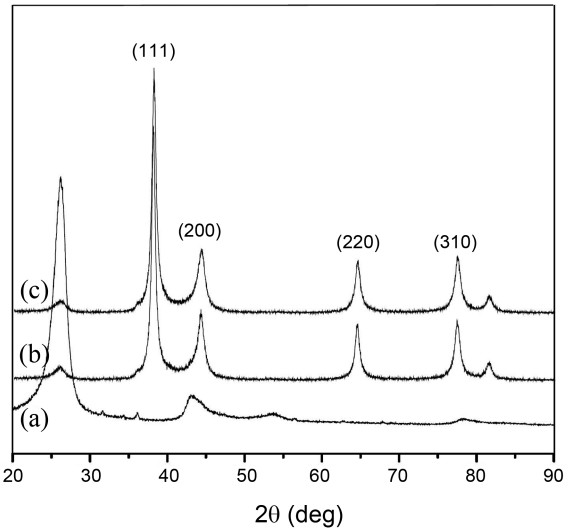

Figure 2. XRD patterns of (a) pristine MWCNTs and (b) MWCNT-Ag and (c) MWCNT-Ag-NH_2.

thermally decomposed at only about 230 °C, in the very early stage compared to that of pristine MWCNTs (at about 430 °C). The differences in the decomposition temperature of MWCNT-bodies for the both samples may be due to the catalytic activity of Ag-NPs for the thermal decomposition. The weight loss of MWCNT-Ag below 400 °C, about 83% of the organic part, showed the significantly different decomposition time as well, when compared to that of pristine MWCNTs, only about 4%. In the case of MWCNT-Ag-NH_2, the primary and secondary weight loss at 130 and 435 °C due to the decompositions of the aminoethanthiol moiety and carbon nanotube body, respectively, were clearly observable. The differences in the decomposition temperature of MWCNT-bodies for the three samples also may be resulted from the different catalytic activities of naked and organic compound-covered Ag-NPs with respect to thermally degradable MWCNTs. The attached silver contents, estimated from the residual weight of the functionalized samples at 800 °C, are 59% and 50% for the nanohybrid

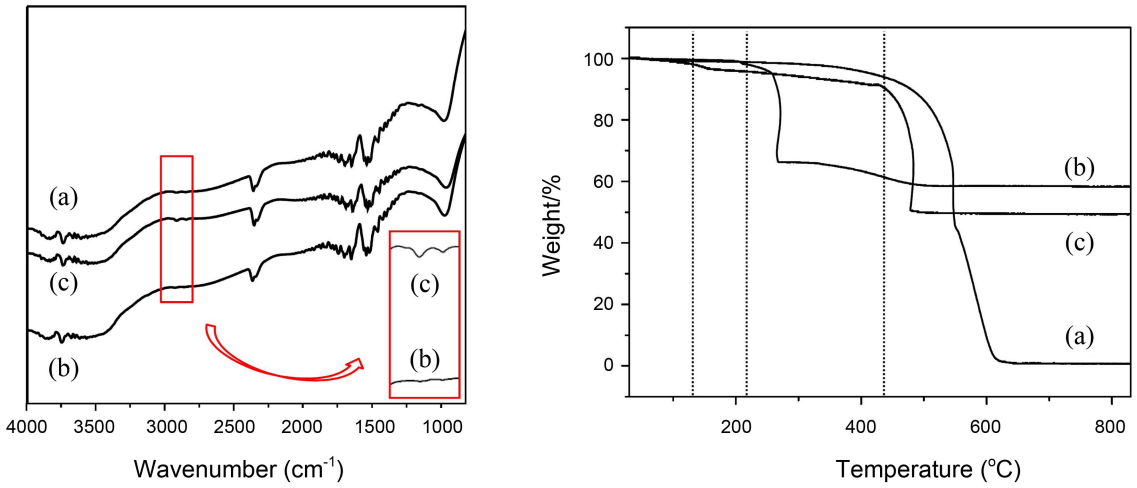

Figure 3. FTIR spectra (left) and TGA data (right) of (a) pristine MWCNTs, (b) MWCNT-Ag and (c) MWCNT-Ag-NH_2.

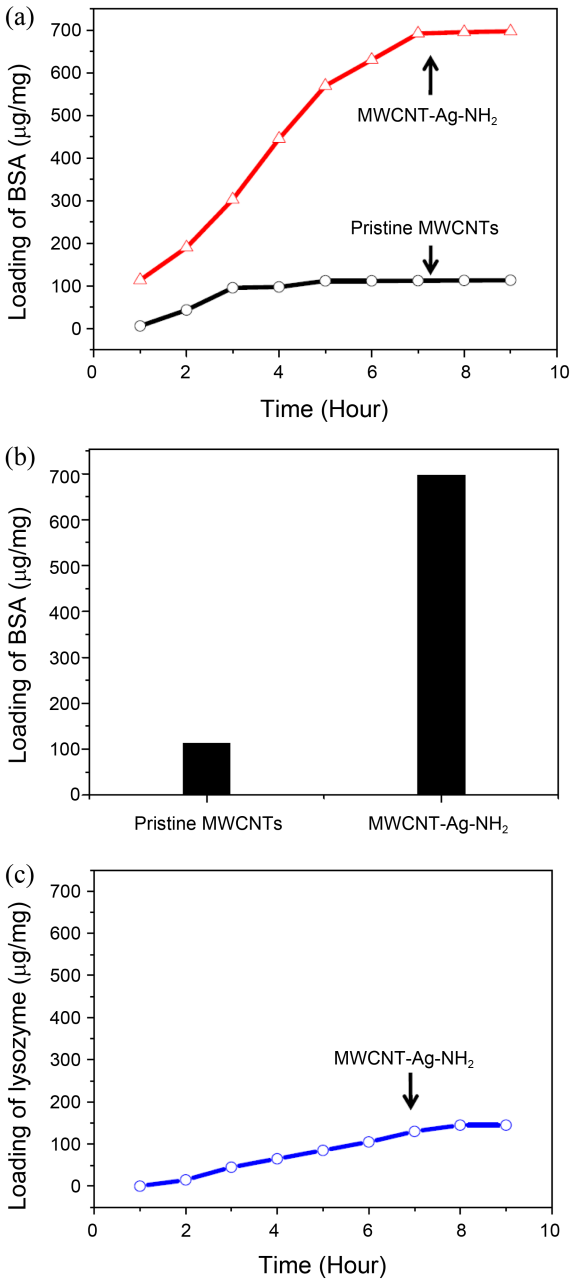

Figure 4. (a) BSA loading kinetics on pristine MWCNTs and MWCNT-Ag-NH_2 hybrid, (b) maximum adsorption capacities of pristine MWCNTs and MWCNT-Ag-NH_2 in the equilibrium state; (c) Lysozyme loading kinetics on MWCNT-Ag-NH_2 hybrid.

products, MWNT-Ag and MWCNT-Ag-NH_2, respectively. The efficacy of the MWCNT-Ag-NH_2 hybrid in loading and delivery of biomolecules was demonstrated using protein bovine serum albumin (BSA; Sigma-Aldrich).[24,25] The protein loading and delivery studies were conducted using UV-vis spectrometer (Shimadzu, UV-1601PC). Figure 4 shows the adsorption kinetics of BSA either on the pristine MWCNTs or on the silver- and amine-functionalized MWCNT derivative, MWCNT-Ag-NH_2. On the MWCNTs the BSA adsorption increased for 3 h and then slowed to a plateau. On the other hand, the BSA adsorption of the MWCNT-Ag-NH_2 occurred continually for up to 6 h. The

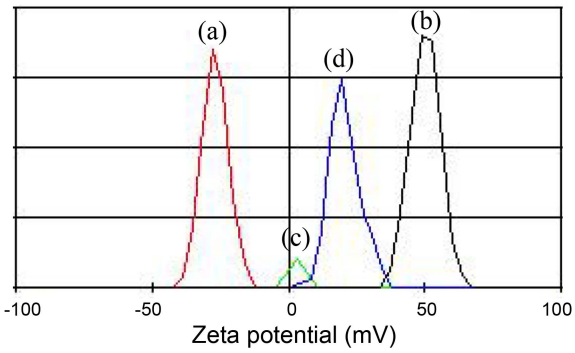

Figure 5. Zeta potential distribution of (a) pristine MWCNTs, (b) MWCNT-Ag-NH_2, (c) BSA, and (d) lysozyme.

BSA adsorption of the MWCNT-Ag-NH_2 was significantly higher than that of the MWCNTs, showing the maximum adsorption level of MWCNT-Ag-NH_2 and pristine MWCNTs per one mg of the sample being 697 and 113 μg, respectively (Figure 4(b)). This BSA loading was associated with the charge-charge interaction between negatively charged BSA molecule and the positively charged surface of the nanohybrid. As another model protein, lysozyme (Sigma-Aldrich), which is known to be highly positively-charged, was also compared the loading behavior onto the nanohybrid, MWCNT-Ag-NH_2 (Figure 2(c)). Although the adsorption of lysozyme onto the MWCNT-Ag-NH_2 was shown to increase slightly with time, the adsorption amount was much lower than the case of BSA, being similar to the case of BSA onto pristine MWCNT. We measured the Zeta (ξ) potential of pristine MWCNTs, the MWCNT-Ag-NH_2, BSA, and lysozyme to observe the surface charge difference. The Zeta (ξ) potential of aqueous solutions of the samples was recorded by Zetasizer nano ZS90 (Malvern) at room temperature and pH = 7.0. The value is automatically calculated from electrophoretic mobility based on the Smoluchowski equation, $v = (\varepsilon E/\eta)\xi$, where v is the measured electrophoretic velocity, η is the viscosity, ε is the electrical permittivity of the electrolytic solution and E is the electric field. As shown in Figure 3, the Zeta (ξ) potential of BSA and lysozyme which are known to be negatively- and positively-charged, respectively, was recorded to be −0.504 and +20.5 mV. On the other hand, as expected, the amine-functionalized MWCNT nanohybrid, MWCNT-Ag-NH_2, gave a positive value of +50.1 mV which highly shifted from a negative value of −26.7 mV of pristine MWCNTs. The results clearly demonstrate the fact that the high efficacy of the amine-functionalized MWCNT nanohybrid for the protein adsorption came from the charge-charge interaction between negatively charged BSA molecule and the positively charged surface of the MWCNT-Ag-NH_2 nanohybrid. The specific binding behavior and high binding capacity of the positively charged MWCNT-Ag-NH_2 strongly suggest the potential usefulness of the current system for the delivery of negatively charged biomolecules including genes and growth factors. The BSA bound to the MWCNT-Ag-NH_2 hybrid was further released in phosphate buffer solution (PBS, pH 7.0, GIBCO Invitro-

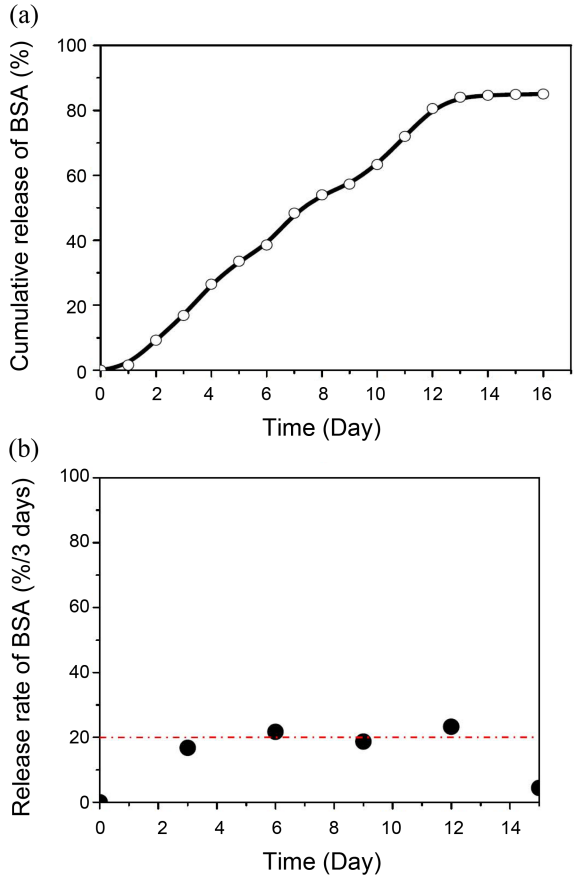

Figure 6. (a) BSA release kinetics and (b) release rate from MWCNT-Ag-NH_2 hybrid.

gen Corporation) at 37 °C for a period of up to 16 days. The cumulative release kinetics of BSA is shown in Figure 6(a). Surprisingly, the release profile was almost linear without showing an initial burst release. This release pattern will be ideal for the sustained and controllable release of drugs. During the first 3 days, BSA release was about 20% of the BSA amount initially-loaded on the MWCNT-Ag-NH_2 hybrid, namely about 7% per day. The initial release rate was maintained over the course of about 12 days (Figure 6(b)). From the 13th day, the rate fell below 4%/day and after the 14th day, only a trace amount of protein was released. As a result, the total protein amount released for 16 days was about 83%. It is clear that the protein release was dominated by a reaction-controlled mechanism, showing a linear release profile with time. The mechanism of adsorption and release of protein might be associated with a possible reaction, ion exchange, between BSA and MWCNT-Ag-NH_2 within PBS condition. When BSA molecules meet the MWCNT-Ag-NH_2 nanohybrid, a complex of $[\text{MWCNT-Ag-NH}_3]_n^+[\text{BSA}]_n^-$ might be formed. Probably the complex exchanges its anions (BSA) with anions existing in PBS solution and the ion exchange can occur continuously with time. Based on the results on the specific binding of protein and its further sustained release profile, the MWCNT-Ag-NH_2 hybrid nanomaterials are considered to be potentially useful as a novel delivery system of biomolecules such as proteins and genes. Further works on using specific therapeutic molecules as well as the assessment of tissue and cell compatibility are currently underway.

Conclusion

Ag-NP-immobilized and amine-functionalized multi-walled carbon nanotubes, MWCNT-Ag-NH_2, were prepared to ascertain their augmented capacity for the ionically specific binding with macromolecules such as proteins and genes. For this, Ag-NPs (about 20 nm and 100 nm, respectively, in size and at interval) firstly formed on MWCNTs were further functionalized with 2-aminoethanthiol, to create binding sites with proteins. As expected, the positively functionalized CNT platforms, MWCNT-Ag-NH_2, showed 7 times higher adsorption capacity for bovine serum albumin with negative surface charge compared to that of pristine MWCNTs, as well as the ability to release BSA molecules at almost constant rate for about two weeks in PBS buffer solution. This study demonstrated the potential usefulness of the MWCNTs in conjunction with Ag-NPs for the delivery of biomolecules including negatively-charged proteins and genes.

Acknowledgments. This work was supported by Priority Research Centers Program (grant#: 2009-0093829), WCU (World Class University) program (grant#: R31-10069) and Strategic Technology Project (grant# 10031791) through the National Research Foundation (NRF) funded by the Ministry of Education, Science and Technology and the Ministry of Knowledge Economy.

References and Notes

1. Baughman, R. H.; Zakhidov, A. A.; de Heer, W. A. *Science* **2002**, *297*, 787.
2. Zanello, L. P.; Zhao, B.; Hu, H.; Haddon, R. C. *Nano Letters* **2006**, *6*, 562.
3. Foldvari, M.; Bagonluri, M. *Nanomedicine* **2008**, *4*, 183.
4. Bahr, J. L.; Yang, J.; Kosynkin, D. V.; Bronikowski, M. J.; Smalley, R. E.; Tour, J. M. *J. Am. Chem. Soc*. **2001**, *123*, 6536.
5. Mickelson, E. T.; Huffman, C. B.; Rinzler, A. G.; Smalley, R. E.; Hauge, R. H.; Margrave , J. L. *Chem. Phys. Lett*. **1998**, *296*, 188.
6. Chen, J.; Hamon, M. A.; Hu, H.; Chen, Y.; Rao, A. M.; Eklund, P. C.; Hadron, R. C. *Science* **1998**, *2*, 95.
7. Yu, B.; Zhou, F.; Liu, G.; Liang, Y.; Huck, W. T. S.; Liu, W. *Chem. Commun*. **2006**, *22*, 2356.
8. Rao, A. M.; Eklund, P. C.; Bandow, S.; Thess, A.; Smalley, R. E. *Nature* **1997**, *388*, 257.
9. Penicaud, A.; Poulin, P.; Derre, A.; Anglaret, E.; Petit, P. *J. Am. Chem. Soc*. **2005**, *127*, 8.
10. Liu, C. M.; Cao, H. B.; Li, Y. P.; Xu, H. B.; Zhang, Y. *Carbon* **2006**, *44*, 2919.
11. Jung, D. H.; Kim, B. H.; Lim, Y. T.; Kim, J. W.; Lee, S. Y.; Jung, H. T. *Carbon* **2010**, *48*, 1070.
12. Shen, M.; Wang, S. H.; Shi, X.; Chen, X.; Huang, Q.; Elijah, J. P.; Roger, A. P.; James, R. B., Jr.; Walter, J. W., Jr. *J. Phys. Chem. C* **2009**, *113*, 3150.
13. Guo, Y.; Guo, S.; Fang, Y.; Dong, S. *Electrochimica Acta* **2010**, *55*, 3927.
14. Arora, S.; Jain, J.; Rajwade, J. M.; Paknikar, K. M. *Toxicol. Appl. Pharmacol*. **2009**, *236*, 310.

15. Niu, A.; Han, Y.; Wu, J.; Yu, N.; Xu, Q. *J. Phys. Chem. C* **2010**, *114*, 12728.
16. Kalishwaralal, K.; BarathManiKanth, S.; Pandian, S. R. K.; Deepak, V.; Gurunathan, S. *J. Control. Release* **2010**, *145*, 76.
17. Miura, N.; Shinohara, Y. *Biochem. Biophys. Res. Commun*. **2009**, *390*, 733.
18. Lewinski, N.; Colvin, V.; Drezek, R. *Small* **2008**, *4*, 26.
19. Gopinath, P.; Gogoi, S. K.; Sanpui, P.; Paul, A.; Chattopadhyay, A. *Colloids Surf. B* **2010**, *77*, 240.
20. Wang, J.; Rahman, M. F.; Duhart, H. M.; Newport, G. D.; Patterson, T. A. *et al*. *Neurotoxicology* **2009**, *30*, 926.
21. Jeon, Y. M.; Cho, H. N.; Gong, M. S. *Macromol. Res*. **2009**, *17*, 2.
22. Lim, T. H.; Jeon, Y. M.; Gong, M. S. *Polymer (Korea)* **2009**, *33*, 33.
23. Hong, H. K.; Gong, M. S.; Park, C. K. *Bull. Korean Chem. Soc*. **2009**, *30*, 2669.
24. Hong, H. K.; Park, C. K.; Gong, M. S. *Bull. Korean Chem. Soc.* **2010**, *31*, 1252.
25. Park, H. S.; Park, H. S.; Gong, M. S. *Polymer (Korea)* **2010**, *34*, 144.
26. Park, H. S.; Park, H. S.; Gong, M. S. *Bull. Korean Chem. Soc*. **2010**, *31*, 2575.
27. Park, H. S.; Park, H. S.; Gong, M. S. *Macromol. Res*. **2010**, *18*, 897.
28. Park, H. S.; Shin, U. S.; Kim, H. W.; Gong, M. S. *Bull. Korean Chem. Soc.* **2011**, *32*, 273.
29. Hong, H. K.; Shin, U. S.; Kim, H. W.; Gong, M. S. *Bull. Korean Chem. Soc.* **2011**, *32*, 1583.